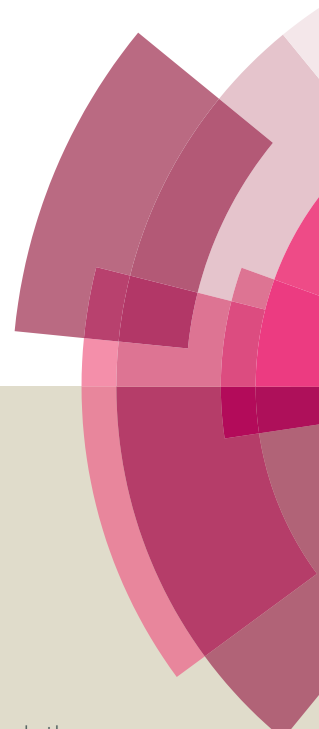


Catalysis Science & Technology

Accepted Manuscript



This article can be cited before page numbers have been issued, to do this please use: K. Shimizu, K. Kon, S. Takakusagi and W. Onodera, *Catal. Sci. Technol.*, 2014, DOI: 10.1039/C4CY00757C.



This is an *Accepted Manuscript*, which has been through the Royal Society of Chemistry peer review process and has been accepted for publication.

Accepted Manuscripts are published online shortly after acceptance, before technical editing, formatting and proof reading. Using this free service, authors can make their results available to the community, in citable form, before we publish the edited article. We will replace this *Accepted Manuscript* with the edited and formatted *Advance Article* as soon as it is available.

You can find more information about *Accepted Manuscripts* in the [Information for Authors](#).

Please note that technical editing may introduce minor changes to the text and/or graphics, which may alter content. The journal's standard [Terms & Conditions](#) and the [Ethical guidelines](#) still apply. In no event shall the Royal Society of Chemistry be held responsible for any errors or omissions in this *Accepted Manuscript* or any consequences arising from the use of any information it contains.

Hydrodeoxygenation of fatty acids and triglyceride by Pt-loaded Nb₂O₅ catalysts

Kenichi Kon^a, Wataru Onodera,^a Satoru Takakusagi,^a Ken-ichi Shimizu^{a,b,*}

^a Catalysis Research Center, Hokkaido University, N-21, W-10, Sapporo 001-0021, Japan

^b Elements Strategy Initiative for Catalysts and Batteries, Kyoto University, Katsura, Kyoto 615-8520, Japan

*Corresponding author

Ken-ichi Shimizu

Catalysis Research Center, Hokkaido University, N-21, W-10, Sapporo 001-0021, Japan

E-mail: kshimizu@cat.hokudai.ac.jp, Fax: +81-11-706-9163

Abstract

Platinum nanoparticles loaded onto various supports have been studied for the selective hydrogenation of lauric acid to *n*-dodecane. The activity depends on the support material and pre-reduction temperature. Pt/Nb₂O₅ reduced at 300 °C gives the highest activity. Pt/Nb₂O₅ shows higher activity than Nb₂O₅-supported various transition metals (Ir, Re, Ru, Pd, Cu, Ni). Under solvent-free conditions Pt/Nb₂O₅ is effective for hydrodeoxygenation of lauric, capric, palmitic, myristic, oleic, and stearic acids under 8 bar H₂ at 180-250 °C, which gives high yield (88-100%) of linear alkanes with the same chain length as the starting compound. Tristearin is also converted to give 93% yield of *n*-octadecane. Pt/Nb₂O₅ shows more than 60 times higher turnover number (TON) than the previously reported catalysts for hydrogenation of stearic acid to *n*-octadecane. Mechanistic study shows a consecutive reaction pathway in which lauric acid is hydrogenated to 1-dodecanol, which undergoes esterification with lauric acid as well as hydrogenation to *n*-dodecane. The ester undergoes hydrogenolysis to give the alcohol, which is hydrogenated to the alkane. Infrared (IR) study of acetic acid adsorption on Nb₂O₅ indicates that Lewis acid-base interaction of Nb cation and carbonyl oxygen, suggesting a possible role of Nb₂O₅ as activation site of carbonyl groups during the hydrodeoxygenation.

Introduction

Developing alternative fuels from non-food biomass has become a key factor to ensure the sustainable growth through minimizing the carbon footprint. In this context, triglyceride and fatty acids have been identified as promising resources of bio-diesel,¹⁻⁵ because they can be easily and economically produced from microalgae which has rapid growth rate and high lipid content. As comprehensively reviewed by Murzin et al.,² three upgrading processes, cracking, transesterification and deoxygenation, have been developed to produce bio-diesel. Deoxygenation of triglyceride/fatty acid feed under hydrogen is of particular importance, because the reaction reduces high-oxygen content and related acidity of fatty acids, yielding saturated hydrocarbons suitable for drop-in diesel fuel. As comprehensively described by Lercher et al.¹ and Bitter et al.³ catalytic deoxygenation of biomass-derived fatty acid derivatives can be classified into three reactions: decarbonylation, decarboxylation and hydrodeoxygenation. Decarbonylation and decarboxylation yield hydrocarbons with one carbon

atom less than the fatty acids, while hydrodeoxygenation gives hydrocarbons with the same chain length as the starting compound. Hydrodesulfurization catalysts (sulfided CoMo or NiMo oxides), which are selective to hydrodeoxygenation,^{6,7} can suffer from sulfur leaching. In contrast, most of the supported group 9 and 10 metal catalysts,⁸⁻¹⁵ such as Ni/ZrO₂⁸ and supported Pd, Pt, and Rh catalysts,⁹⁻¹³ suffer from high selectivity to decarbonylation or decarboxylation products even in the presence of H₂. A few catalysts (Ni-loaded zeolites,¹⁶ Pt-Re/ZSM-5,¹⁷ and tungsten and molybdenum carbides¹⁸⁻²¹) have been reported to be effective for selective transformation of fatty acids into diesel-range alkanes without a loss of the chain length of the corresponding fatty acid at 260-350 °C under 10-50 bar H₂. However, they have still problems such as high catalyst loading (low turnover number, TON), formation of small amount of decarbonylation and cracking byproducts and needs of high pressure H₂ and high temperature. In this paper we report selective and quantitative hydrodeoxygenation of stearic acid to *n*-octadecane under milder conditions (180 °C, 2 or 8 bar H₂) than previous studies using Pt/Nb₂O₅, which shows more than two orders of magnitude higher TON than Pt/SiO₂ and previous catalysts for the selective hydrodeoxygenation of fatty acids. Substrate scope, kinetic and in situ IR studies are also carried out to discuss the catalytic performance, reaction pathways, and a possible role of Nb₂O₅ in the present catalytic system.

Experimental

General

Commercially available organic compounds (from Tokyo Chemical Industry or Kanto Chemical) were used without further purification. The GC (Shimadzu GC-14B) and GCMS (Shimadzu GCMS-QP2010) analyses were carried out with Ultra ALLOY capillary column UA⁺-1 (Frontier Laboratories Ltd.) using nitrogen and He as the carrier gas.

Catalyst preparation

Nb₂O₅ (54 m² g⁻¹) was prepared by calcination of niobic acid (Nb₂O₅·nH₂O, kindly supplied by CBMMI) at 500 °C for 3 h. SiO₂ (Q-10, 300 m² g⁻¹) was supplied from Fuji Silysia Chemical Ltd. H⁺-type MFI zeolite (HMFI) with a SiO₂/Al₂O₃ ratio of 22.3 was kindly supplied by Tosoh Co. HBEA zeolite (JRC-Z-HB25, SiO₂/Al₂O₃= 25±5), silica-alumina (JRC-SAL-2, SiO₂/Al₂O₃=5.6), MgO (JRC-MGO-3), TiO₂ (JRC-TIO-4), CeO₂ (JRC-CEO-3) was supplied from Catalysis Society of Japan. γ-Al₂O₃ was prepared by calcination of γ-AlOOH (Catapal B Alumina purchased from Sasol) for 3 h at 900 °C. ZrO₂ was prepared by calcination (500 °C for 3 h) of ZrO₂·nH₂O prepared by hydrolysis of zirconium oxynitrate 2-hydrate in water by aqueous NH₄OH solution, followed by filtration of precipitate, washing with water three times, and drying at 100 °C.

Precursor of Pt/Nb₂O₅ was prepared by an impregnation method; a mixture of Nb₂O₅ and an aqueous HNO₃ solution of Pt(NH₃)₂(NO₃)₂ was evaporated at 50 °C, followed by drying at 90 °C for 12 h. Before each catalytic experiment, the Pt/Nb₂O₅ catalyst (with Pt loading of 5 wt%) was prepared by in situ pre-reduction of the precursor in a pyrex tube under a flow of H₂ (20 cm³ min⁻¹) at 300 °C for 0.5 h. Other supported Pt catalysts (Pt = 5 wt%) were prepared by the same method. Nb₂O₅-supported metal catalysts, M/Nb₂O₅ (M = Ni, Cu, Ru, Pd, Ag, Re, Ir) with metal loading of 5 wt% were prepared by impregnation method in the similar manner as Pt/Nb₂O₅ using aqueous solution of metal nitrates (for Co, Ni, Cu, Ag), RuCl₃, IrCl₃·nH₂O, NH₄ReO₄ or aqueous HNO₃ solution of Pd(NO₃)₂. A commercial Pt-loaded carbon catalyst

(Pt/C, Pt = 5 wt%) was purchased from N.E. Chemcat, Corporation.

Characterization

The temperature programmed reduction under H₂ (H₂-TPR) was carried out with BELCAT (BELL Japan Inc.). Unreduced precursor of Pt/Nb₂O₅, Pt(NH₃)₂(NO₃)₂-loaded Nb₂O₅ (20 mg), was mounted in a quartz tube, and the sample was heated with a temperature ramp-rate of 2 °C min⁻¹ in a flow of 5% H₂/Ar (20 cm³ min⁻¹). The effluent gas was passed through a trap containing MS4Å to remove water, then through the thermal conductivity detector. The amount of H₂ consumed during the experiment was detected by a thermal conductivity detector.

The number of surface metal atoms in Pt/Nb₂O₅, pre-reduced in H₂ at 300 °C for 0.5 h, was estimated from the CO uptake of the samples at room temperature using the pulse-adsorption of CO in a flow of He by BELCAT. The average particle size was calculated from the CO uptake assuming that CO was adsorbed on the surface of spherical Pt particles at CO/(surface Pt atom) = 1/1 stoichiometry.

TEM measurements were carried out by using a JEOL JEM-2100F TEM operated at 200 kV.

In situ IR spectra were recorded using a JASCO FT/IR-4200 equipped with an MCT detector. For the IR studies of CO and pyridine adsorption, we used a flow-type IR cell connected to a flow reaction system. For the IR study of acetic acid adsorption, we used a closed IR cell connected to an evacuation system. The sample was pressed into a 40 mg of self-supporting wafer ($\phi = 2$ cm) and mounted into the IR cell with CaF₂ windows. Spectra were measured accumulating 15 scans at a resolution of 4 cm⁻¹. A reference spectrum of the catalyst wafer in He taken at measurement temperature was subtracted from each spectrum. For the CO-IR study, a disk of Pt/Nb₂O₅ was heated in H₂ flow (20 cm³ min⁻¹) at 300 °C for 0.5 h, followed by exposure to a flow of CO(5%)/He (20 cm³ min⁻¹) for 180 s at 40 °C, and by purging with He for 600 s. Then, IR measurement was carried out. For the pyridine-IR study, the Pt/Nb₂O₅ disc, pre-reduced in H₂ at 300 °C for 0.5 h, was exposed to 1 μ L of liquid pyridine vaporized at 200 °C under He flow at 150 °C. Then, the disk was purged with He for 600 s, and IR measurement was carried out. During the acetic acid-IR study, the IR cell was cooled by an ice bath, and the thermocouple near the sample showed 8 ± 1 °C. The sample disc (Nb₂O₅ or SiO₂) in the closed IR cell, pre-evacuated at 500 °C for 0.5 h, was exposed to 20 Pa of acetic acid at 8 °C for 600 s, then IR spectra were measured at 8 °C.

Typical procedures of catalytic reactions

Pt/Nb₂O₅ (0.07, 0.2 or 1 mol%-Pt with respect to carboxylic acid) pre-reduced at 300 °C was used as a standard catalyst. The other catalysts were also pre-reduced at 300 °C before reaction. After the pre-reduction, the catalyst in the closed glass tube sealed with a septum inlet was cooled to room temperature under H₂ atmosphere. The mixture of carboxylic acid (1 mmol) and *n*-decane or *n*-dodecane (0.2 mmol) was injected to the pre-reduced catalyst inside the glass tube through the septum inlet. Then, the septum was removed under air, and a magnetic stirrer was put in the tube, followed by inserting the tube inside stainless autoclave with a dead space of 28 cm³. Soon after being sealed, the reactor was flushed with H₂ from a high pressure gas cylinder and charged with H₂ (typically 8 bar) at room temperature. Then, the reactor was heated typically at 180 °C under stirring (150 rpm). After the reaction, acetone (10 cm³) was added to the mixture, and conversion and yields of products were determined by GC using *n*-decane or *n*-dodecane as an internal standard. The products were identified by GC-MS

equipped with the same column as GC and by comparison with commercially available products.

Results and discussion

Characterization of Pt/Nb₂O₅

We characterized the structure of the representative catalyst, Pt/Nb₂O₅ pre-reduced at 300 °C. H₂-TPR of the unreduced precursor, Pt(NH₃)₂(NO₃)₂-loaded Nb₂O₅, is shown in Fig. 1. The H₂ consumption due to the reduction of oxidic Pt to metallic Pt is observed mostly below 100 °C. Fig. 2 shows the particle size distribution of Pt/Nb₂O₅ obtained by transmission electron microscopy (TEM) analysis. The volume-area mean diameter of Pt particle was 4.7 nm. The number of exposed Pt⁰ sites estimated by the CO adsorption amount (28.3 μmol g⁻¹-cat) is smaller than the number of the surface Pt atoms (39.4 μmol g⁻¹-cat) estimated by using the volume-area mean diameter of Pt by TEM and by assuming that CO is adsorbed on the surface of spherical Pt particles at a stoichiometry of CO/(surface Pt atom) = 1/1. This result is consistent with the previous result that increase in the H₂-treatment temperature of Pt/Nb₂O₅ leads to decrease in hydrogen and CO uptake on the catalyst.²²⁻²⁴ This phenomenon has been generally called strong metal-support interaction (SMSI),²²⁻³⁴ where a metal surface is partially covered with suboxide (NbOx) species produced by partial reduction of the support (Nb₂O₅) at high temperature (200-500 °C). The SMSI phenomenon was also observed in Nb₂O₅-supported Pd, Rh and Ir catalysts.²⁶⁻²⁸ The IR study of CO adsorption on Pd/Nb₂O₅ showed that increase in the reduction temperature of Pd/Nb₂O₅ from 100 °C to 300 °C resulted in the suppressions of the band at 1938 cm⁻¹ due to the bridged CO on Pd.²⁷ This observation was assigned to the blocking of the Pd surface by migrated NbOx species. As shown in Fig. 3, our IR experiments of CO adsorption on Pt/Nb₂O₅ gave similar results. The IR spectrum of CO on Pt/Nb₂O₅ reduced at 100 °C showed bands in a range 2000-2080 cm⁻¹ due to linearly coordinated CO on Pt⁰ and a band at 1840 cm⁻¹ due to bridged CO on flat surface of Pt.²⁴ The increase in the reduction temperature of Pt/Nb₂O₅ from 100 °C to 300 °C resulted in the large suppression of the bridged CO band and the linear CO bands (especially at low wavenumber region). The result supports the SMSI model of Pt/Nb₂O₅ reduced at 300 °C, where the Pt surface is partly covered with NbOx species. Summarizing the structural results, it is concluded that the dominant Pt species in Pt/Nb₂O₅ pre-reduced at 300 °C are Pt metal particles whose surface is partially covered with NbOx species.

Optimization of catalysts and conditions

We studied the influence of various catalyst parameters on the catalytic activity for hydrogenation of lauric acid in solvent-free conditions under 8 bar H₂ at 180 °C for 4 h using 1 mol% of the catalyst (Table 1). First, various metal (M)-loaded Nb₂O₅ catalysts (M= Pt, Ir, Ru, Re, Pd, Cu, Ni), pre-reduced at 300°C, were studied (entries 2-8). It was found that Pt/Nb₂O₅ showed the highest yield of n-dodecane. 1-Dodecanol and dodecyl dodecanoate were also produced as byproducts. Next, we screened a series of supported Pt catalysts pre-reduced at 300°C (entries 2,10-20). The activity depended strongly on the support materials, and Pt/Nb₂O₅ (entry 2) showed more than 10 times higher yield of n-dodecane (60%) than the other Pt-loaded metal oxides (entries 10-20). Pt/TiO₂ (entry 13) and niobic acid-supported Pt (entry 10) also showed high conversion, but these catalysts gave partially reduced products (dodecyl dodecanoate and 1-dodecanol) as main products. Pt metal particles on an inert support (Pt/SiO₂,

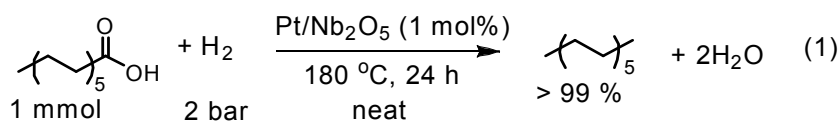
entry 12) and Nb₂O₅ itself (entry 1) showed no yield of dodecane, indicating that Pt metal particles and the support itself could not catalyze the reaction under the present conditions. The Pt/Nb₂O₅ catalyst reduced at 100 °C (entry 9) showed lower yield of n-dodecane (16%) than that reduced at 300 °C (60%).

With the most effective catalyst, Pt/Nb₂O₅ reduced at 300 °C, we studied the optimization of reaction conditions. Fig. 4 shows the effect of hydrogen pressure on conversion and product yields for the reaction after 4 h. Note that the conversion and yield at H₂ pressure of 0 bar correspond to the reaction under 1 bar N₂. The dodecane yield was highest at H₂ pressure of 8 bar. Further increase in the H₂ pressure decreased the yield of dodecane and increased those of dodecanol and ester. This may suggest a competitive activation of hydrogen and lauric acid at the same catalytic site under high H₂ pressure.

Fig. 5 shows the time course of the reaction under solvent-free conditions at 180 °C in 8 bar H₂. Note that the conversion and yield at *t* = 0 h were measured after addition of the reaction mixture to the pre-reduced Pt/Nb₂O₅ under ambient conditions. The profile is characteristic to consecutive reaction mechanism; 1-dodecanol and dodecyl dodecanoate, formed at an initial induction period, were consumed after 1 h to give the over-hydrogenated product, n-dodecane. After 24 h, the yield of n-dodecane was 99%, and no formation of byproducts was observed by GC-MS analysis. Next, we tested the reaction under 8 bar H₂ for 24 h in different solvents (Table 2). The reaction under solvent-free conditions gave the highest yield (99%) of n-dodecane. The reaction in toluene also gave good yield (90%). Use of *o*-xylene, mesitylene, diglyme and water resulted in moderate yield (31-43%) with co-production of 1-dodecanol and dodecyl dodecanoate as byproducts.

Performance of Pt/Nb₂O₅-catalyzed hydrogenation of fatty acids

From the above optimization experiments, we found the best conditions (8 bar H₂, 24 h, 180 °C, 1 mol% Pt/Nb₂O₅, without solvent), which gave a quantitative dodecane yield without any byproducts (Table 3, entry 1). ICP-AES analysis of the solution after the reaction confirmed that the contents of Pt and Nb in the solution were below the detection limits. After the standard reaction for 24 h, the catalyst was separated from reaction mixture by centrifugation and was dried at 90 °C at 12 h and then reduced in H₂ at 300 °C for 0.5 h. The recovered catalyst showed quantitative yield of n-dodecane (Table 3, entries 2,3). These results indicate that Pt/Nb₂O₅ acts as reusable heterogeneous catalysts for this reaction. It is important to note that this system is effective even under low H₂ pressure of 2 bar, giving a quantitative yield (equation 1).



As summarized in Table 3, the scope of the liquid-phase hydrogenation using Pt/Nb₂O₅ under solvent-free conditions was further expanded to various fatty acids and tristearin. The reactions of capric, palmitic, myristic, oleic, and stearic acids at low hydrogen pressure (8 bar) at 180-250 °C resulted in high yield (88-99%) of linear alkanes with the same chain length as the starting compound, and yields of byproducts (lower or branched alkanes, alcohols and esters) were below the detection limit of GC analyses. Tristearin was also converted to give 93% yield

of n-octadecane. Another important aspect of this catalytic system is high TON. As shown in entry 8, hydrogenation of 2 mmol stearic acid in the presence of small amount of the catalyst (0.07 mol%) at 250 °C under 8 bar H₂ resulted in 96% yield of n-octadecane, corresponding to TON of 1371 with respect to total number of Pt atoms in the catalyst. As compared in Table 4, this value is more than 60 times higher than those of previously reported heterogeneous catalysts. Under the same conditions, Pt/SiO₂ gave no yield of n-octadecane but gave 7% yield of a hydrocarbon with one carbon atom less than the fatty acids.

Reaction pathways

The kinetic profile for hydrogenation of lauric acid (Fig. 5) indicates the consecutive reaction pathway; dodecanol and dodecyl dodecanoate, formed at an initial induction period, are hydrogenated to yield dodecane as the final product. To give further evidences on the tentative mechanism, we compared the initial rates of the individual steps. Table 5 lists the initial formation rates of the products for hydrogenation of lauric acid, 1-dodecanol, 1-dodecanol or dodecyl dodecanoate (ester), together with the ester formation rate by the reaction of lauric acid with 1-dodecanol. For the hydrogenation of lauric acid, the formation of n-dodecane (5 mmol h⁻¹) is slower than the formation of 1-dodecanol (17 mmol h⁻¹) and the ester (31 mmol h⁻¹). The hydrogenation of 1-dodecanol, 1-dodecanol and dodecyl dodecanoate resulted in the formation of n-dodecane as the main product. The order of the n-dodecane formation rate is as follows: dodecanol (15 mmol h⁻¹) > dodecanol (13 mmol h⁻¹) > dodecyl dodecanoate (8 mmol h⁻¹) > lauric acid (5 mmol h⁻¹). Considering the facts that the esterification of lauric acid with 1-dodecanol (63 mmol h⁻¹) shows the highest rate in the reactions in Table 5, we propose a possible reaction pathway in Scheme 1. The carboxylic acid is hydrogenated to an alcohol possibly via an aldehyde. However, the fact that 1-dodecanol is not produced by the hydrogenation of 1-dodecanol (entry 2 in Table 5) suggests a direct hydrogenation of carboxylic acid to alcohol. The alcohol undergoes esterification with the carboxylic acid as well as hydrogenation to an alkane (dodecane). The ester undergoes hydrogenolysis to give the alcohol, which is hydrogenated to the alkane. During the model hydrogenation of dodecanol (Table 5, entry 2), we did not observe dodecene as a byproduct, which exclude a possible formation of dodecane via dehydration of the alcohol to alkene followed by its hydrogenation. The proposed pathway in Scheme 1 is consistent with that proposed by Lercher for the catalytic hydrogenation of stearic acid to octadecane over Ni/HBA catalyst.¹⁶ They proposed the production of octadecane by the consecutive pathway: stearic acid hydrogenation to 1-octadecanol, followed by 1-octadecanol hydrogenation to octadecane.

Possible role of Nb₂O₅

As discussed above, Pt/Nb₂O₅ showed significantly higher activity than the other Pt-loaded catalysts and Nb₂O₅ itself, suggesting a synergy between Pt and the Nb₂O₅ support. On the basis of our characterization results and the SMSI model of the Pt/Nb₂O₅ system in the literatures,²²⁻²⁴ we have concluded that that the dominant Pt species in the most effective catalyst, Pt/Nb₂O₅ reduced at 300 °C, are the Pt metal particles whose surface is partly covered with NbOx species. As shown in Table 1, increase in the reduction temperature of Pt/Nb₂O₅ from 100 °C to 300 °C increased its activity for the hydrodeoxygenation. The CO-IR result in Fig. 3 suggests that increase in the reduction temperature of Pt/Nb₂O₅ from 100 °C to 300 °C resulted in nearly complete blocking of the bridged site on a flat Pt surface by NbOx species. Summarizing these

results, the higher activity of the Pt/Nb₂O₅ catalyst reduced at 300 °C is explained by a partial decoration of Pt by NbOx in which relatively large number of Pt⁰ atoms can be located at metal-NbOx perimeter sites. Pt/TiO₂ is also well known as a SMSI catalyst.²⁹⁻³⁴ Table 1 shows that Pt/TiO₂ (reduced at 300 °C) is a moderately effective catalyst; it shows higher yields of dodecane and partially reduced products (dodecyl dodecanoate and dodecanol) than non-SMSI catalysts (such as Pt/C, Pt/SiO₂ and Pt/Al₂O₃). These facts lead to a hypothesis that cooperation between Pt metal and adjacent NbOx (or TiOx) species is responsible for the high catalytic activity.

It is known that the partial blocking of Pt by suboxides (NbOx or TiOx) causes the formation of new perimeter sites between Pt and the suboxide.²²⁻²⁴ Yoshitake and Iwasawa²² studied hydrogenation of acrolein by the Pt/Nb₂O₅ catalyst in SMSI state (reduced at 500 °C). They propose that the higher selectivity in C=O bond reduction than C=C bond reduction is caused by a cooperation between Pt and NbOx at the perimeter sites, in which H₂ is dissociated by Pt and acrolein is activated by NbOx. Vannice²⁹ also showed a significant enhancement in the selectivity in C=O bond reduction for hydrogenation of crotonaldehyde by Pt/TiO₂ reduced at 500 °C. Somorjai and Bell showed that activity of Rh foil for CO and CO₂ hydrogenation was increased by partially decorating the Rh surface with suboxides such as NbOx, and the activity for the decorated Rh surface increased with increase in the Lewis acidity of the suboxide.³⁷ This rate enhancement is attributed to the activation of the C=O bond via Lewis acid-base interaction between the cationic sites in the suboxide and the oxygen atom of CO or CO₂.³⁷⁻³⁹ Enhanced selectivity or activity by metal-Lewis acid cooperation at metal-oxide interface has been reported for various catalytic systems for hydrogenation of C-O or C=O bonds.^{22,26-31,35-43}

As evidenced by the IR band due to coordinated pyridine on Lewis acid site (1445 cm⁻¹) in the pyridine adsorption IR experiment (Fig. 6), Pt/Nb₂O₅ has Lewis acid sites (exposed Nbⁿ⁺ cations). Then, to evaluate the Lewis acid-base interaction between Nb cations and carbonyl oxygens of carboxylic acids in the present system, we carried out IR observation of acetic acid on Nb₂O₅. The spectrum in Fig. 7 shows the C=O stretching band of adsorbed acetic acid³⁰ at lower wavenumber (1660 cm⁻¹) than that for non Lewis acidic oxide, SiO₂ (1715 cm⁻¹). This indicates charge transfer from the oxygen atom of carboxyl group (Lewis base) to the Nb⁵⁺ cation (Lewis acid) site of the Nb₂O₅ surface. Taking these discussions into consideration, we propose that polarization of the C=O bond of carboxylic acid by Lewis acid-base interaction of the Nb cation and carboxyl group is the primary important role of the Nb₂O₅ support in the present catalytic system (Scheme 2). The high activity of Pt/Nb₂O₅ can be caused by cooperation between Pt and NbOx at the perimeter sites, in which H₂ is dissociated by Pt and carboxylic acid is activated by NbOx via the Lewis acid-base interaction. The increase in the activity with increase in the reduction temperature of Pt/Nb₂O₅ from 100 °C to 300 °C could be explained by an increase in the Pt-NbOx perimeter length caused by a migration of NbOx islands onto Pt metal surface.

Conclusions

Pt/Nb₂O₅ was found to be an effective catalyst for hydrodeoxygenation of lauric, capric, palmitic, myristic, oleic, and stearic acids at low H₂ pressure (8 bar) at 180-250 °C under solvent-free conditions, which gives high yield of linear alkanes with the same chain length as the starting compound. Tristearin is also converted to give 93% yield of *n*-octadecane under 50

bar H₂ at 260 °C. Pt/Nb₂O₅ shows more than 60 times higher TON than previously reported catalysts for hydrogenation of stearic acid to *n*-octadecane. Mechanistic study showed the following reaction pathways. Carboxylic acid is hydrogenated to alcohol, which undergoes esterification with carboxylic acid as well as hydrogenation to alkane. The ester undergoes hydrogenolysis to give alcohol, which is hydrogenated to alkane. Pt/Nb₂O₅ in a partial SMSI state showed significantly higher activity than the non-SMSI catalysts. Combined with the IR evidence on the Lewis acid-base interaction between the surface Nb cation and carboxyl oxygen of an adsorbed carboxylic acid, we propose that the high activity of Pt/Nb₂O₅ is caused by cooperation between Pt and NbOx at the perimeter sites, in which H₂ is dissociated by Pt and carboxylic acid is activated by NbOx via the Lewis acid-base interaction.

Acknowledgement

This work was supported by a Grant-in-Aid for Scientific Research on Innovative Areas "Nano Informatics" (25106010) from JSPS and a MEXT program "Elements Strategy Initiative to Form Core Research Center".

Notes and references

1. C. Zhao, T. Brück and J. A. Lercher, *Green Chem.*, 2013, **15**, 1720–1739.
2. S. Lestari, P. Mäki-Arvela, J. Beltramini, G. Q. Max Lu and D. Yu. Murzin, *ChemSusChem*, 2009, **2**, 1109–1119.
3. R. W. Gosselink, S. A. Hollak, S.-W. Chang, J. van Haveren, K. P. de Jong, J. H. Bitter and D. S. van Es, *ChemSusChem*, 2013, **6**, 1576–1594.
4. F. Shi, P. Wang, Y. H. Duan, D. Link and B. Morreale, *RSC Adv.*, 2012, **2**, 9727–9747.
5. J. C. Serrano-Ruiz, E. V. Ramos-Fernandez and A. Sepulveda-Escribano, *Energy Environ. Sci.*, 2012, **5**, 5638–5652.
6. O. I. Senol, E. M. Ryymin, T. R. Viljava and A. O. I. Krause, *J. Mol. Catal. A*, 2007, **268**, 1–8.
7. Y. Liu, R. Sotelo-Boyas, K. Murata, T. Minowa and K. Sakanishi, *Energy Fuels*, 2011, **25**, 4675–4685.
8. B. Peng, C. Zhao, S. Kasakov, S. Fortaita and J. A. Lercher, *Chem. Eur. J.*, 2013, **19**, 4732–4741.
9. I. Kubičková, M. Snåre, K. Eränen, P. Mäki-Arvela and D. Yu. Murzin, *Catal. Today*, 2005, **106**, 197–200.
10. B. Rozmysłowicz, P. Mäki-Arvela, A. Tokarev, A.-R. Leino, K. Eränen and D. Y. Murzin, *Ind. Eng. Chem. Res.*, 2012, **51**, 8922–8927.
11. J. Han, H. Sun, Y. Ding, H. Lou and X. Zheng, *Green Chem.*, 2010, **12**, 463–467.
12. J. Han, H. Sun, J. Duan, Y. Ding, H. Lou and X. Zheng, *Adv. Synth. Catal.*, 2010, **352**, 1805–1809.
13. C. Wang, Z. Tian, L. Wang, R. Xu, Q. Liu, W. Qu, H. Ma and B. Wang, *ChemSusChem*, 2012, **5**, 1974–1983.
14. M. Snåre, I. Kubičková, K. Eränen, P. Mäki-Arvela and D. Yu. Murzin, *Ind. Eng. Chem. Res.*, 2006, **45**, 5708–5715.
15. P. Mäki-Arvela, I. Kubičková, M. Snåre, K. Eränen and D. Yu. Murzin, *Energy Fuels*, 2007, **21**, 30–41.

16. B. Peng, Y. Yao, C. Zhao and J. A. Lercher, *Angew. Chem., Int. Ed.*, 2012, **51**, 2072–2075.
17. K. Murata, Y. Liu, M. Inaba and I. Takahara, *Energy Fuels*, 2010, **24**, 2404–2409.
18. R. W. Gosselink, D. R. Stellwagen and J. H. Bitter, *Angew. Chem., Int. Ed.*, 2013, **52**, 5089–5092.
19. S. A. W. Hollak, R. W. Gosselink, D. S. van Es and J. H. Bitter, *ACS Catal.*, 2013, **3**, 2837–2844.
20. J. Han, J. Duan, P. Chen, H. Lou, X. Zheng and H. Hong, *Green Chem.*, 2011, **13**, 2561–2568.
21. J. X. Han, J. Z. Duan, P. Chen, H. Lou and X. M. Zheng, *Adv. Synth. Catal.*, 2011, **353**, 2577–2583.
22. H. Yoshitake and Y. Iwasawa, *J. Catal.*, 1990, **125**, 227–242.
23. D. A. G. Aranda, A. L. D. Ramos, F.B. Passos and M. Schmal, *Catal. Today*, 1996, **28**, 119–125.
24. D. A. G. Aranda and M. Schmal, *J. Catal.* 171, 1997, 398–405.
25. S. J. Tauster, S. C. Fung and R. L. Garten, *J. Am. Chem. Soc.*, 1978, **100**, 170–171.
26. H. Yoshitake, K. Asakura and Y. Iwasawa, *J. Chem. Soc., Faraday Trans., 1*, 1989, **85**, 2021–2024.
27. A. Maeda, F. Yakamawa, K. Kunimori and T. Uchijima, *Catal. Lett.*, 1990, **4**, 107–112.
28. T. Uchijima, *Catal. Today*, 1996, **28**, 105–117.
29. A. Dandekar and M. A. Vannice, *J. Catal.*, 1999, **183**, 344–354.
30. W. Rachmady and M. A. Vannice, *J. Catal.*, 2002, **207**, 317–330.
31. P. Reyes, M.C. Aguirre, I. Melian-Cabrera, M. Lopez Granados and J. L. G. Fierro, *J. Catal.*, 2002, **208**, 229–237.
32. J. Sa, J. Bernardi and J. A. Anderson, *Catal. Lett.*, 2007, **114**, 91–95.
33. V. A. D. O'Shea, M. C. A. Galvan, A. E. P. Parts, J. M. Campos-Martin and J. L. G. Fierro, *Chem. Commun.*, 2011, **47**, 7131–7133.
34. S. Bonanni, K. Aït-Mansour, H. Brune and W. Harbich, *ACS Catal.*, 2011, **1**, 385–389.
35. T. Iizuka, Y. Tanaka and K. Tanabe, *J. Mol. Catal.*, 1982, **17**, 381–389.
36. M. A. Vannice, *Catal. Today*, 1992, **12**, 255–267.
37. A. Boffa, C. Lin, A. T. Bell and G. A. Somorjai, *J. Catal.*, 1994, **149**, 149–158.
38. A. T. Bell, *J. Mol. Catal. A*, 1995, **100**, 1–11.
39. Y. Borodko and G. A. Somorjai, *Appl. Catal. A*, 1999, **186**, 355–362.
40. P. M. Maitlis and V. Zanolib, *Chem. Commun.*, 2009, **45**, 1619–1634.
41. Y. Nakagawa, M. Tamura and K. Tomishige, *ACS Catal.*, 2013, **3**, 2655–2668.
42. D. A. Ruddy, J. A. Schaidle, J. R. Ferrell III, J. Wang, L. Moens and J. E. Hensley, *Green Chem.*, 2014, **16**, 454–490.
43. S. Nishiyama, T. Hara, S. Tsuruya and M. Masai, *J. Phys. Chem. B*, 1999, **103**, 4431–4439.

Table 1. Hydrogenation of lauric acid by 5 wt% metal-loaded catalysts.

Entry	Catalyst	Conv. (%)	Yield (%)		
			dodecane	dodecanol	ester ^a
1	Nb ₂ O ₅	29	0	0	0
2	Pt/Nb ₂ O ₅	100	60	7	21
3	Ir/Nb ₂ O ₅	86	19	12	31
4	Ru/Nb ₂ O ₅	73	4 (8) ^c	9	29
5	Re/Nb ₂ O ₅	23	1	0	4
6	Pd/Nb ₂ O ₅	21	1	0	4
7	Cu/Nb ₂ O ₅	24	1	0	0
8	Ni/Nb ₂ O ₅	23	0.4	0	0
9	Pt/Nb ₂ O ₅ ^b	93	16	11	36
10	Pt/niobic acid	98	13	19	24
11	Pt/C	2	1	0	0
12	Pt/SiO ₂	1	0	0	0
13	Pt/TiO ₂	82	6	13	41
14	Pt/SiO ₂ -Al ₂ O ₃	42	3	0	1
15	Pt/BEA	8	2	0	2
16	Pt/MFI	61	1	0	1
17	Pt/ZrO ₂	14	2	0	9
18	Pt/Al ₂ O ₃	14	1	0	1
19	Pt/CeO ₂	2	1	0	2
20	Pt/MgO	44	1	3	0

^a dodecyl dodecanoate.^b Pre-reduced at 100 °C for 0.5 h.^c undecane

Table 2. Hydrogenation of lauric acid by Pt/Nb₂O₅.^a

Solvent	Conv.(%)	Yield (%)		
		n-dodecane	1-dodecanol	ester ^b
Solvent-free	100	99	0	0
toluene	100	90	9	2
<i>o</i> -xylene	100	42	12	39
mesitylene	100	31	17	45
diglyme	100	43	17	40
H ₂ O	97	40	49	10

^a Conditions: lauric acid (1 mmol), catalyst (1 mol%), solvent (0.2 g), 180 °C, 8 bar H₂, 24 h.^b dodecyl dodecanoate.**Table 3.** Hydrogenation of fatty acids by Pt/Nb₂O₅.^a

Entry	fatty acid	Pt (mol%)	<i>T</i> (°C)	<i>t</i> (h)	Conv. (%)	Yield (%)		
						<i>n</i> -C _{<i>n</i>} H _{2<i>n</i>+2} ^b	alcohol	ester
1	Lauric acid	1	180	24	100	99	0	0
2 ^c		1	180	24	100	99	0	0
3 ^d		1	180	24	100	99	0	0
4	Capric acid	1	180	24	100	88	0	0
5	Palmitic acid	0.2	250	24	100	90	0	0
6	Myristic acid	0.2	250	24	100	89	0	0
7	Oleic acid	0.2	250	24	100	99	0	0
8 ^e	Stearic acid	0.07	250	48	100	96	0	0
9 ^f	Tristearin	1	260	24	100	93	0	0

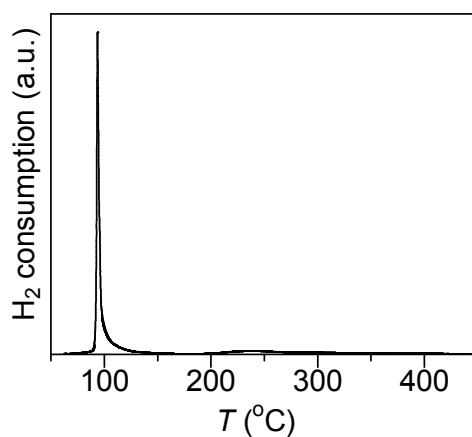
^a 1 mmol fatty acid, solvent-free, 8 bar H₂.^b Linear alkanes with the same chain length as the starting compound.^c 1st reuse.^d 2nd reuse.^e 2 mmol stearic acid, 8 bar H₂.^f 1 mmol tristearin, 50 bar H₂, 1 mol% Pt cat. with respect to carboxyl group.

Table 4. Heterogeneous catalysts for hydrogenation of stearic acid to octadecane.^a

Catalyst	mol%	<i>T</i> (°C)	<i>t</i> (h)	<i>P</i> _{H₂} (bar)	Yield (%)	TOF (h ⁻¹)	TON	ref.
Pt/Nb ₂ O ₅	0.07	250	48	8	96	29	1371	this study ^a
Pt/SiO ₂	0.07	250	48	8	0 (7) ^b	-	-	this study ^a
Ni/HBEA	9.65	260	8	40	97.3	1.3	10	16
Mo ₂ C/C	22.3	280	4	10	75	3.4	0.8	21
W-based cat.	2.9	350	5	50	67	4.6	23	18

^a Conditions: 2 mmol stearic acid, solvent-free, 8 bar H₂.^b Yield of *n*-heptadecane.**Table 5.** Hydrogenation of model compounds by Pt/Nb₂O₅.^a

Entry	Substrate	Initial rate / mmol h ⁻¹		
		<i>n</i> -dodecane	1-dodecanol	ester ^b
1	lauric acid	5	17	31
2	1-dodecanal	15	0	-
3	1-dodecanol	13	-	-
4	ester ^b	8	0	-
5 ^c	esterification	-	-	63

^a Conditions: 1 mmol substrate, solvent-free, 1 mol% Pt catalyst, 180 °C, 8 bar H₂.^b dodecyl dodecanoate.^c Esterification of lauric acid (1 mmol) with 1-dodecanol (1 mmol) at 180 °C in 1 atm N₂.**Fig. 1** H₂-TPR profile for unreduced precursor of Pt/Nb₂O₅.

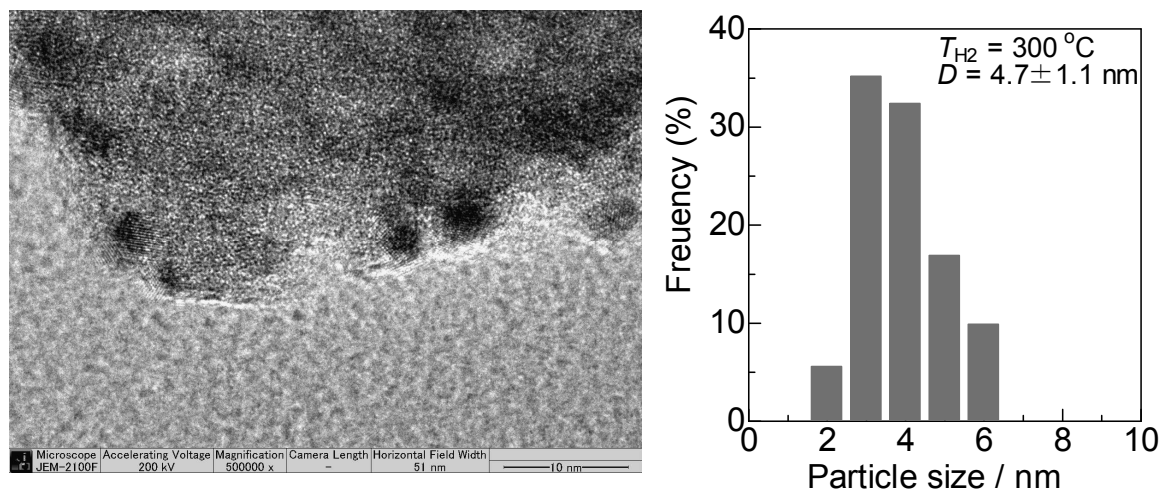


Fig. 2 A representative TEM image and Pt particle size distribution of Pt/Nb₂O₅ (pre-reduced at 300 °C). The volume-area mean diameter of Pt particle was 4.7 ± 1.1 nm.

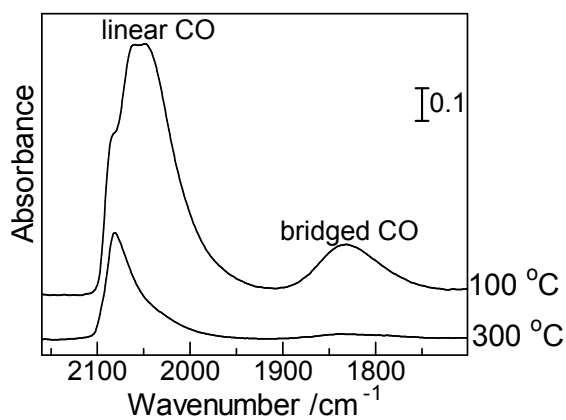


Fig. 3 IR spectra (40 °C) of CO adsorbed on Pt/Nb₂O₅ pre-reduced at 100 and 300 °C.

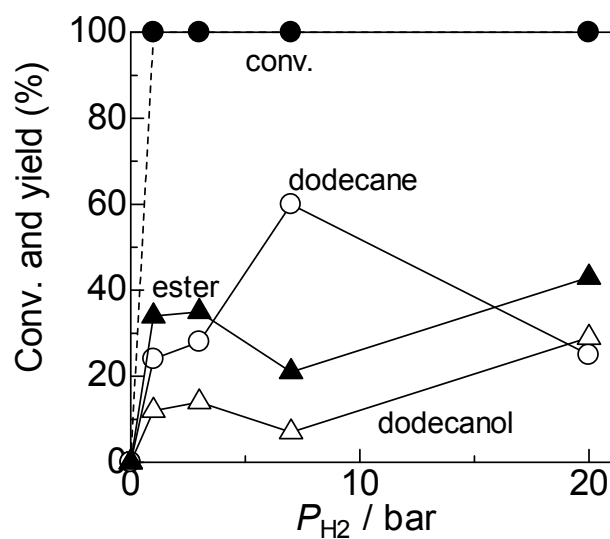


Fig. 4 Effect of H_2 pressure on conversion and products yields for lauric acid hydrogenation by Pt/Nb_2O_5 (pre-reduced at $300\text{ }^\circ\text{C}$).

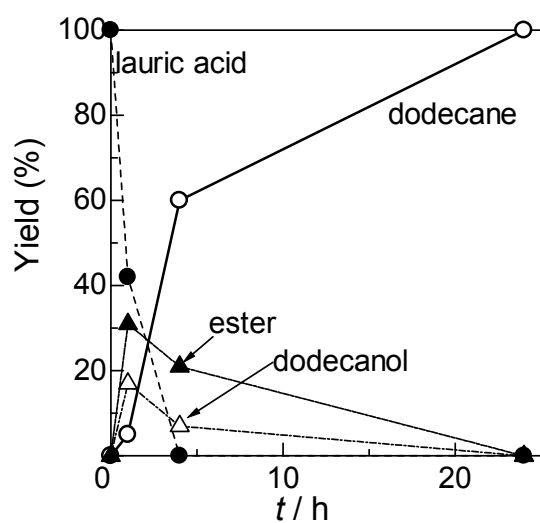


Fig. 5 Time-conversion profile for lauric acid hydrogenation by Pt/Nb_2O_5 (pre-reduced at $300\text{ }^\circ\text{C}$).

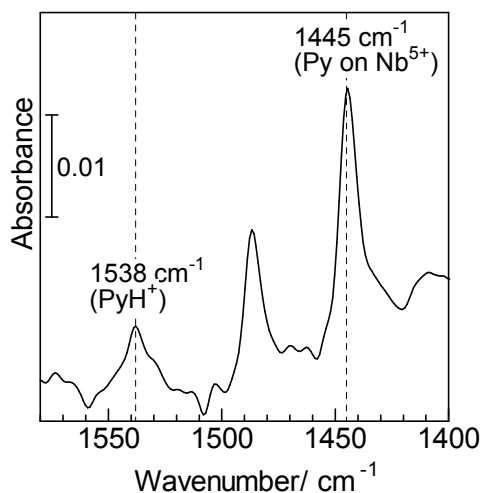


Fig. 6 IR spectra of pyridine adsorbed on Pt/Nb₂O₅ at 150 °C.

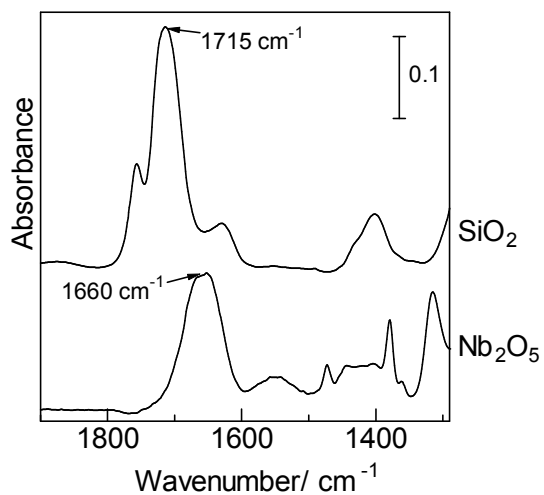
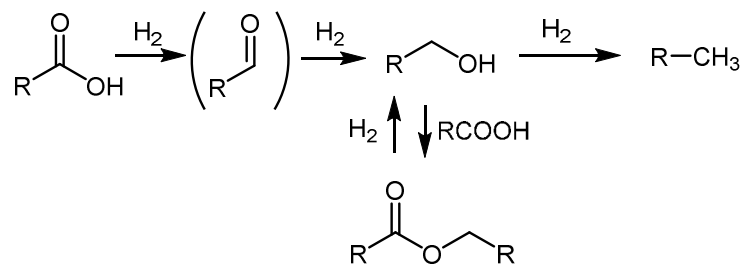
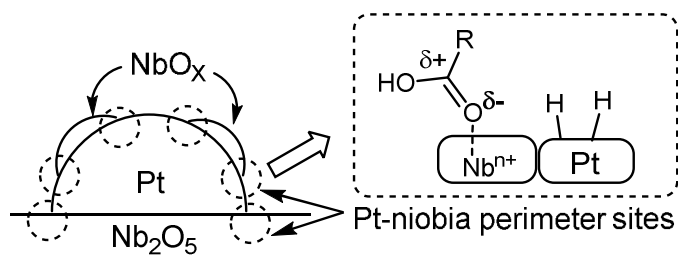


Fig. 7 IR spectra of acetic acid adsorbed on Nb₂O₅ and SiO₂ at 8 °C.



Scheme 1 Proposed reaction pathway for hydrodeoxygenation of lauric acid by Pt/Nb₂O₅.



Scheme 2 Proposed cooperative mechanism of hydrodeoxygenation of carboxylic acids by Pt/Nb₂O₅ in a partially SMSI state.

Table of Contents

Pt/Nb₂O₅ shows more than 60 times higher TON than non-SMSI Pt catalysts and previous catalysts for hydrodeoxygenation of stearic acid to *n*-octadecane at 180 °C in 8 bar H₂. Nb₂O₅ can act as activation sites of carbonyl groups.

